Feasibility Study of Monitoring Railway Bridges Using Axle Box Accelerations: A Joint Analysis of Simulations and Field Measurements

Willem Simon Wolswijk[1(✉)], Yuanchen Zeng[1], Stefan Verdenius[2], Jurjen Hendriks[1], Milan Veljkovic[1], and Zili Li[1]

[1] Department of Engineering Structures, Delft University of Technology, Stevinweg 1, 2628CN Delft, The Netherlands
w.s.wolswijk-1@tudelft.nl

[2] Unit of Mobility and Built Environment, TNO, Delft, The Netherlands

Abstract. Ensuring the safety and longevity of railway bridges requires efficient, non-invasive methods for monitoring their health and detecting structural damage. Drive-by health monitoring (DBHM) has emerged as a promising approach, using vehicle-mounted sensors, such as axle box acceleration (ABA), to assess the structural integrity of bridges. This method offers the advantage of frequent monitoring under operational conditions. However, DBHM faces challenges in real-world applications due to the subtle influence of local damage and disturbances like vehicle dynamics, track irregularities, and noise. This study investigates the feasibility of using ABA to detect structural damage in a real railway bridge. Continuous wavelet transforms and filtering techniques are used to isolate different vibration components within ABA signals. A finite element model of a cracked beam is developed, and simulations reveal that local structural damage introduces a small, local peak in the quasi-static ABA component. Field measurements show the variability of ABA measurements over space and time and the resulting difficulty in directly detecting the local damage. However, probabilistic analysis suggests that reference signals under healthy conditions, combined with frequent monitoring, can enhance the reliability of damage detection using DBHM.

Keywords: Drive-by health monitoring · Railway bridge · Axle box acceleration · Finite element analysis · Damag localisation

1 Introduction

Traditionally, bridge health monitoring has relied on visual inspections and, in some cases, on structural health monitoring (SHM) systems that utilise sensors installed on the bridge. While providing valuable information, such systems often involve high costs, complex installations, and significant maintenance efforts [1].

Á. Cunha and E. Caetano (Eds.): EVACES 2025, LNCE 676, pp. 360–369, 2025.
https://doi.org/10.1007/978-3-031-96114-4_38

Drive-by health monitoring (DBHM) offers a cost-effective alternative by equipping vehicles with accelerometers to capture axle box acceleration (ABA) signals as they traverse a bridge, with the signals reflecting potential bridge damage bridge. This eliminates the need for effort-intensive on-site sensor installations, allowing a few sensor-equipped vehicles to monitor entire rail networks.

The potential of DBHM has been demonstrated in simulated environments, detecting significant structural damage exceeding stiffness losses of 20% over several meters [2–6]. Recent studies have refined the approach by decomposing ABA signals into quasi-static and dynamic components, finding that the quasi-static component offers greater potential for detecting and localising damage [3]. Changes in the quasi-static component are localised to the area of damage, while changes in dynamic components such as bridge natural frequencies affect the ABA over a larger portion of the bridge, hindering damage localisation.

However, challenges remain in understanding how structural damage manifests in ABA signals under real-world conditions where noise, environmental factors, and operational variability can impact the accuracy of damage detection [1]. Considering that most studies rely on simulations or scaled models [7–9], the feasibility of DBHM in practical applications is yet to be thoroughly validated, leaving a critical gap in confirming its robustness for large-scale deployment.

This paper addresses these gaps by integrating detailed finite element simulations with field measurements. Using a case study of a railway bridge, the research first uses simulations to examine how local structural damage affects the axle box acceleration signals of passing trains. Combining these simulations with field measurements, it then evaluates the feasibility of DBHM to detect and localise damage under real-world conditions, providing insights into its practical application. The research examines the passage of the TU Delft CTO measurement vehicle over a one-track steel bridge with four primary girders of I-section profiles. The bridge consists of two spans, with the first spanning 10 m and the second spanning 13 m. During a visual inspection, a crack was observed in the bottom flange of one of the main girders of the second span, with the crack being present over the entire width of the flange.

The remainder of this paper is structured as follows. Section 2 presents a detailed description of the finite element model used to simulate the quasi-static component of a train's passage, followed by an analysis of the resulting simulation data. In Sect. 3, field measurements are analysed and the results are integrated with the finite element solutions from Sect. 2. Finally, Sect. 4 concludes the study and provides recommendations for further research.

2 Modelling and Simulation of a Cracked Beam

To understand the impact of the crack described in Sect. 1 on the ABA of the train passing the bridge, a finite element model (FEM) of a cracked beam is developed in DIANA FEA. The model consists of one of the four girders from the railway bridge, shown in Fig. 1(a). The beam is made of steel with an elastic modulus of $E = 210$ GPa and Poisson ratio of $\nu = 0.3$, modelled using 2D

flat shell elements with linear interpolation. All supports are modelled as line elements across the bottom flange of the beam.

The crack is modelled by duplicating the nodes at the crack face and removing their connectivity. To accurately capture the beam's behaviour near the crack while minimizing computation, the mesh is refined in this region (Fig. 1(b)). The element sizes near the crack and along the rest of the beam are $b_{\text{crack}} = 0.025$ m and $b_{\text{main}} = 0.1$ m, chosen based on a mesh sensitivity study.

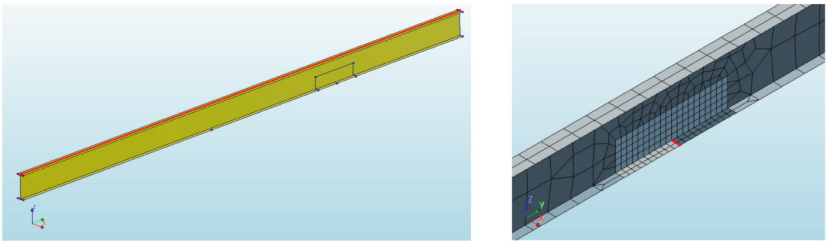

Fig. 1. FEM of the main girder. (a) Overall view. (b) Mesh near the crack.

This model focuses on the quasi-static response, excluding dynamic vehicle-bridge interactions. The train load is simplified as a point load moving along the centreline of the top flange. The vertical displacement of the axle box is thereby equated to the displacement of the beam at the load position. For practicality, one bogie is assumed to act on the bridge, evenly distributed across the four girders, such that each beam carries one-eighth of the train's total weight.

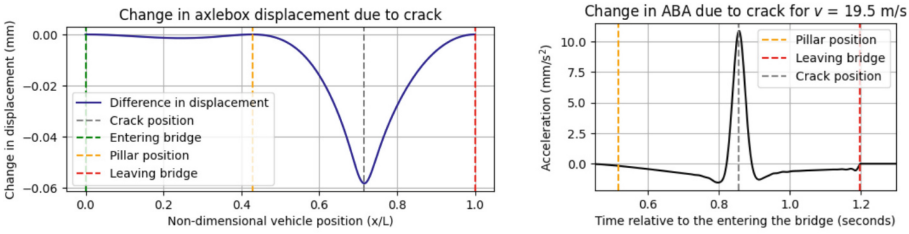

Fig. 2. Influence of the crack on (a) axle box displacement and (b) ABA, for a train speed of $v = 19.5$ m/s, zoomed in on the second span.

Figure 2(a) shows the change in axle box displacement as a result of the crack. The change in ABA between the healthy and damaged case (the "damage component") is extracted by calculating the second derivative with respect to time

using the central difference scheme [10]. Figure 2(b) illustrates this component for a train speed of $v = 19.5$ m/s. Note that while the quasi-static component is speed-independent, its resulting acceleration does depend on the train speed.

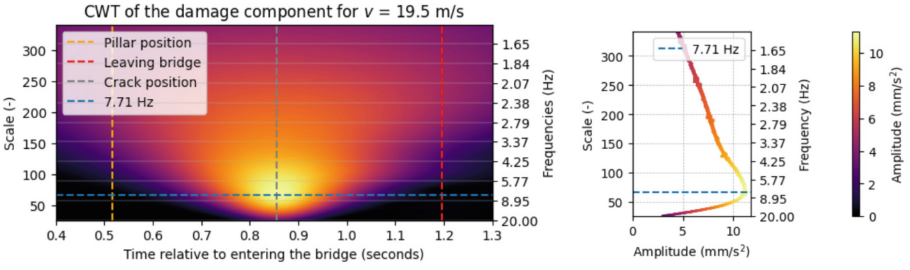

(a) (b)

Fig. 3. Time-frequency domain of the damage component for $v = 19.5$ m/s. (a) CWT. (b) Cut in the CWT at the crack position.

Figure 3(a) shows the time-frequency representation of the damage component using a Continuous Wavelet Transform (CWT). Figure 3(b) shows a cut in the CWT at the position of the crack, which illustrates the frequency contents of the damage component as the axle passes over the crack. As visible, for a train speed of $v = 19.5$ m/s, the frequency most present in the damage component (and thus most impacted by the damage), the so-called "peak frequency", is $f_d \approx 7.71$ Hz. The amplitude of the damage component is $A_d \approx 11$ mm/s^2.

By performing the above process for a range of train speeds, the influence of the train speed on the peak frequency and amplitude of the damage component is evaluated. As shown in Fig. 4, there is a near-linear relationship between the train speed and the peak frequency ($f_d \propto v$) and a quadratic relationship between the train speed and the amplitude of the damage component ($A_d \propto v^2$).

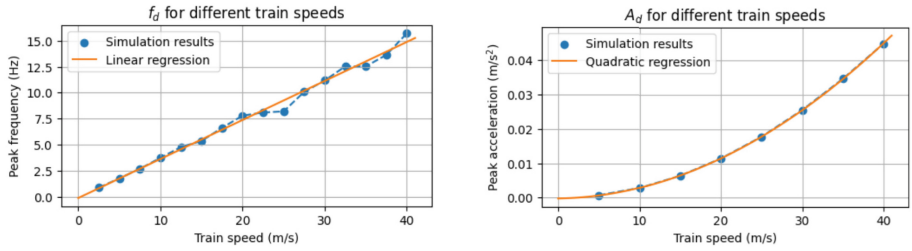

(a) (b)

Fig. 4. Influence of the train speed on the damage component. (a) Influence on the peak frequency (f_d). (b) Influence on the amplitude (A_d)

3 Field Measurements and Damage Detectability

To further assess the effectiveness of DBHM, this section considers field measurements performed on the bridge of the case study. Measurements from three different measurement campaigns are analysed, each consisting of one passage over the bridge using the TU Delft CTO measurement vehicle. Figure 5(a) shows a top view scheme of the CTO vehicle with its eight axle boxes.

The measurement campaigns, M1, M2, and M3 took place in July 2015, December 2015, and May 2023, with train speeds of 12.87 m/s, 19.50 m/s, and 18.73 m/s. During M1, measurements were taken using sensors L1, L2, R1, and R2, while M2 utilized sensors L3, L4, R3, and R4 and M3 utilized all sensors. The bridge was in a healthy state without known damage for all measurements.

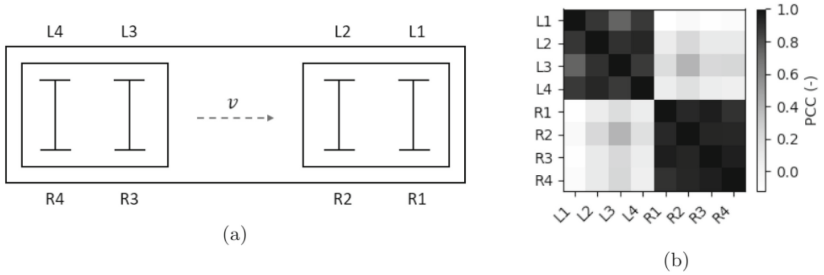

Fig. 5. (a) CTO sensor positions. (b) PCCM for ABA from M3.

As shown in Sect. 2, the considered crack is expected to affect low-frequency vibrations within the ABA. To isolate these contents, the measurements are pre-processed using a lowpass filter with a cut-off frequency of 20 Hz.

Variability Between Axle Boxes Within a Passage. Figure 5(b) shows the Pearson correlation coefficient matrix (PCCM) for the ABA recorded in M3, quantifying the pairwise correlation (r) between signals from sensors on the train as it crossed the bridge, calculated after aligning the signals from different positions to account for time lags. The results show a strong correlation between sensors on the same side of the train, indicating that ABA components below 20 Hz are dominated by spatial factors like track irregularities and quasi-static bridge deflections. This high correlation suggests that measurements from sensors on the same side of the train can be grouped together without major loss of accuracy.

Variability Between Measurement Campaigns. To evaluate the repeatability of the ABA between different measurement campaigns, the ABA signals are first converted to the time-frequency domain through the CWT. Consequently,

the local frequency contents are extracted by performing a vertical "cut" at the time point corresponding to the position where the crack is modelled in the finite element model (but not present in reality), at $y = y_c$.

Figure 6(a) provides the frequency contents at this position for all measurements performed on the left side of the train from M1, M2 and M3. As visible, measurements from the same campaign retrieve similar results, whereas measurements from different campaigns differ more significantly. Besides noise and changes in track and wheel geometry, these differences can be largely attributed to the varying train speed between the three passages: M1 was performed at a significantly lower train speed than the other measurements.

To account for the different train speeds, this research proposes a speed-normalisation approach. This approach consists of scaling the frequency and amplitude of the ABA according to the relationships obtained in Sect. 2.

Note that this transformation only holds for space-dependent components in the signal. While Fig. 5(b) indicates that most components are quasi-static (and thus space-dependent), it does not apply to components with frequencies or amplitudes invariant to train speed, such as bridge and vehicle vibrations.

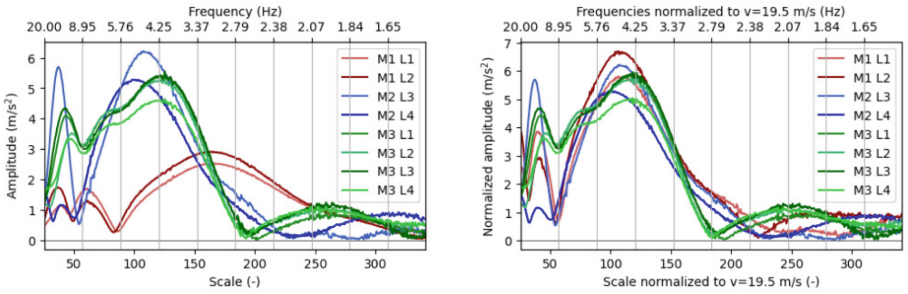

Fig. 6. Frequency contents at the position of interest for ABA measurements on the left side of the train. (a) Frequency contents. (b) Frequency contents after speed normalisation to $v = 19.5$ m/s.

Figure 6(b) shows the frequency contents normalised to a speed of $v = 19.5$ m/s. Normalising the frequency contents improves the consistency between measurements, with M1 aligning closer to the others. However, some variability between them remains, which may affect the detection of local damage.

Quantification of Variability. To stochastically describe the normalised frequency contents above, let us consider the normalised frequency content at a distance y from the start of the bridge and frequency f to be normally distributed such that

$$CWT_{\text{norm}}(y, f) \sim N(\mu_0(y, f), \sigma(y, f)) \tag{1}$$

where CWT_{norm} is the normalized frequency content for a position y and frequency f with mean value $\mu_0(y, f)$ and standard deviation $\sigma(y, f)$, which are estimated by ABA measurements over a large number of train passages.

Figure 7(a) shows the mean of the frequency contents shown in Fig. 6(b). Figure 7(b) presents the corresponding standard deviations, highlighting the variability in frequency strength across different measurements. The standard deviation is notably high between 8–20 Hz on both sides of the train but much lower below 8 Hz, suggesting a lower variability at lower frequencies.

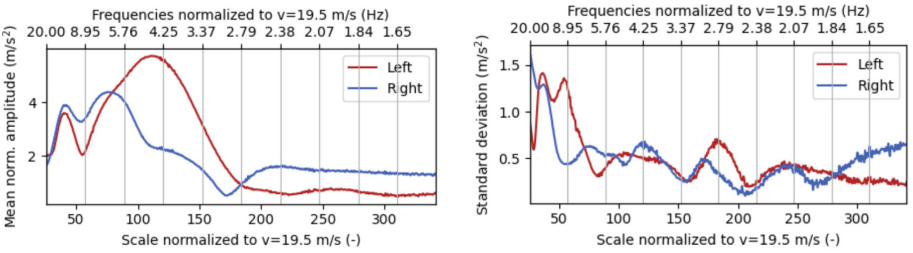

(a) (b)

Fig. 7. Statistical properties of speed-normalised frequency contents at the position of interest. (a) Mean of the amplitude. (b) Standard deviation of the amplitude.

Detectability of Structural Damage. For the purpose of a quantitative evaluation of the detectability, let us assume that the means and standard deviations of Fig. 7 correctly represent the variation in frequency contents of the signal at the position of interest over multiple measurements on the bridge in a healthy state. To perform the probabilistic analysis, a right-tailed test is conducted, with the null and alternative hypotheses defined as follows:

$$H_0 : \mu(y, f) = \mu_0(y, f) \qquad \text{Healthy hypothesis} \qquad (2)$$

$$H_1 : \mu(y, f) > \mu_0(y, f) \qquad \text{Damaged hypothesis} \qquad (3)$$

where the null hypothesis states that the bridge is in a healthy state, such that the mean frequency content (μ) at the position of interest follows the trends indicated in Fig. 7(a). The alternative hypothesis proposes the bridge is damaged, resulting in a greater mean frequency content.

Now let us assume that the local crack discussed in Sect. 2 is present and that it increases the amplitude of the signal in the time-frequency domain in accordance with Fig. 3(a). As such, the mean normalised frequency contents increases in the following manner:

$$\mu(y, f) = \mu_0(y, f) + CWT_{\text{damage}}(y, f) \qquad (4)$$

where $CWT_{\text{damage}}(y, f)$ denotes the amplitude of the CWT of the damage component as shown in Fig. 3(a). At the position of interest, this increases the frequency content with the values shown in Fig. 3(b). The standard deviation of the normalised frequency contents is assumed unchanged by the damage.

To quantify the damage component's amplitude relative to the measurements' natural variation a detectability index $I(y, f)$ is defined, calculated by the ratio of the damage component amplitude to the standard deviation of the measurements ($I(y, f) = \frac{CWT_{\text{damage}}(y,f)}{\sigma(y,f)}$). Figure 8 illustrates the detectability index I at the position of interest as a function of frequency. The frequency at which this ratio peaks corresponds to the frequency where the damage is most noticeable, which occurs at approximately 2.5 Hz.

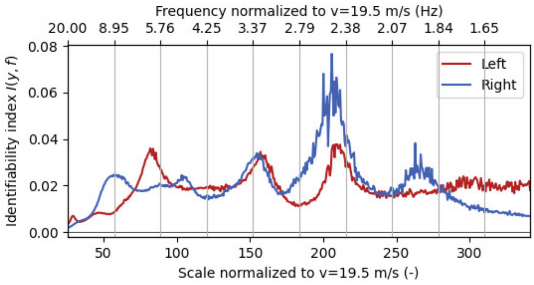

Fig. 8. Detectability index at the position of interest.

In Fig. 8, at 2.5 Hz, the increase in frequency contents due to damage is no more than 7% of the standard deviation in frequency contents between measurements. This demonstrates that the effect of the damage is very subtle in relation to the natural variation of the ABA, suggesting it is not detectable after a single measurement, even with a reference signal.

Nevertheless, DBHM has the advantage of frequently performing measurements on a structure, providing multiple observations over a short time period. This nature has the potential to increase the detectability by collaborating multiple measurements statistically. Consider, therefore, the strategy in which the strength of one specific frequency is monitored at the position of interest ($y = y_c$) over a number of passages N. To determine the number of axle box measurements required to detect the damage reliably, a t-test is performed. For the question at hand, the general definition of the t-test [11] can be reformulated as

$$t(y, f) = \frac{(\mu_0(y, f) + CWT_{\text{damage}}(y, f)) - \mu_0(y, f)}{\frac{\sigma(y,f)}{\sqrt{N}}} = I(y, f) \cdot \sqrt{N} \qquad (5)$$

where $t(y, f)$ is the t-statistic for position y and frequency f. The number of measurements needed to reject the null hypothesis H_0 in favour of H_1 (the bridge is damaged) is therefore

$$N > \left(\frac{Z_{\text{crit}}}{I(y,f)} \right)^2 \tag{6}$$

where Z_{crit} is the critical z-score, which for a confidence level of $\alpha = 0.1$ is equal to $Z_{\text{crit}} = 1.282$. Since the detectability index is found to differ between the left and right sides of the vehicle, the minimum number of axle box measurements to confidently state that the bridge is damaged also differs. Assuming the 2.5 Hz normalised frequency is monitored at the position of interest, this corresponds to $N_{\text{left}} \approx 1825$ measurements for the left hand side of the train and $N_{\text{right}} \approx 657$ measurements for the right hand side.

This number of measurements is not feasible with specially designed measurement trains such as the TU Delft CTO train. However, considering multiple passages of (passenger) trains with ABA sensors on multiple axles, this number of measurements can be performed efficiently within a matter of days.

4 Conclusion

This study assessed the feasibility of using DBHM for railway bridges by analysing the ABA from passing trains to detect structural damage. A case study involving a crack in a bridge girder provided valuable insights into the application of DBHM. The main findings are drawn below.

1. The local structural damage in one of the bridge's main girders causes a localised, sharp increase in the quasi-static component of the ABA, with the amplitude and shape (frequency) depending on train speed.
2. There is a high correlation between measurements on the same side of the train in a single passage, indicating space-dependent vibration components dominate ABA measurements.
3. ABA between different measurement campaigns varies, but a speed normalisation technique that assumes space-dependence improves consistency.
4. The influence of damage on the ABA of a passing vehicle is insignificant compared to the natural variability between measurements. Using a reference signal, combined with a significant number of train passages, can potentially enable effective detection of the damage.

This research investigates a case study involving a rare and exceptionally large damage scenario on a particular railway bridge. In real-world assessments, many factors will affect the detectability results, such as varying train masses and external environmental conditions. Additionally, bridge and track maintenance are likely to change ABA, and their impacts should be clearly distinguished from bridge damage to avoid misinterpretation of changes in ABA.

Much work remains before DBHM can be commercially applied to bridge health monitoring. Further field and controlled laboratory measurements under varying conditions are crucial to better understand the variability of ABA and to improve the method's robustness. Additionally, integrating DBHM with other SHM methods, like acoustic emission monitoring or digital twinning, could provide a more comprehensive bridge health assessment.

Acknowledgement. This paper is based on the first author's MSc Thesis at TU Delft, titled "*Feasibility Study of Railway Bridge Monitoring Using Axlebox Acceleration: A Joint Analysis of Numerical Simulations and Field Measurements.*" The research was completed in 2024 with the support of TNO and under the supervision of TU Delft staff.

References

1. Tan C, Zhao H, Uddin N, Yan B (2022) A fast wavelet-based bridge condition assessment approach using only moving vehicle measurements. Appl Sci (Switzerland) 12(21):11277. https://doi.org/10.3390/app122111277
2. Hester D, González A (2012) A wavelet-based damage detection algorithm based on bridge acceleration response to a vehicle. Mech Syst Signal Process 28:145–166. https://doi.org/10.1016/j.ymssp.2011.06.007
3. Hester D, González A (2017) A discussion on the merits and limitations of using drive-by monitoring to detect localized damage in a bridge. Mech Syst Signal Process 90:234–253. https://doi.org/10.1016/j.ymssp.2016.12.012
4. Carnevale M, Collina A, Peirlinck T (2019) A feasibility study of the drive-by method for damage detection in railway bridges. Appl Sci (Switzerland) 9(1):160. https://doi.org/10.3390/app9010160
5. Tan C, Elhattab A, Uddin N (2017) "Drive-by" bridge frequency-based monitoring utilizing wavelet transform. J Civ Struct Heal Monit 7(5):615–625. https://doi.org/10.1007/s13349-017-0246-3
6. Malekjafarian A, Golpayegani F, Moloney C, Clarke S (2019) A machine learning approach to bridge-damage detection using responses measured on a passing vehicle. Sensors (Switzerland) 19(18):4035. https://doi.org/10.3390/s19184035
7. Corbally R, Malekjafarian A (2023) Detecting changes in the structural behaviour of a laboratory bridge model using the contact-point response of a passing vehicle. J Struct Integrity Maint 4:226–238. https://doi.org/10.1080/24705314.2023.2230399
8. Kim CW, Chang KC, McGetrick PJ, Inoue S, Hasegawa S (2017) Utilizing moving vehicles as sensors for bridge condition screening - a laboratory verification. Sens Mater 29(2):153–163. https://doi.org/10.18494/SAM.2017.1433
9. Zhang B, Zhao H, Tan C, Obrien EJ, Fitzgerald PC, Kim CW (2022) Laboratory investigation on detecting bridge scour using the indirect measurement from a passing vehicle. Remote Sens 14(13):3106. https://doi.org/10.3390/rs14133106
10. Vuik C, Vermolen FJ, van Gijzen MB, Vuik MJ (2015) Numerical methods for ordinary differential equations. TU Delft Open, Delft. https://doi.org/10.5074/t.2023.001
11. Dekking F et al (2005) A modern introduction to probability and statistics. Springer, Delft. https://doi.org/10.1007/1-84628-168-7